Applied Catalysis B: Environmental 327 (2023) 122414

Contents lists available at ScienceDirect

Applied Catalysis B: Environmental

journal homepage: www.elsevier.com/locate/apcatb

Towards a circular economy for Pt catalysts. Case study: Pt recovery from electrodes for hydrogen production

Miguel A. Montiel, Rafael Granados-Fernández, Sergio Díaz-Abad, Cristina Sáez, Carmen M. Fernández-Marchante, Manuel A. Rodrigo, Justo Lobato *

Chemical Engineering Department, University of Castilla-La Mancha, Enrique Costa Novella Building, Av. Camilo Jose Cela n 12, 13004 Ciudad Real, Spain

ARTICLE INFO

Keywords:
ECSA
Electrocatalysts
Hydrogen
Pt
Recovery

ABSTRACT

This work links two challenges that our society is facing nowadays, the climate change and the scarcity of key raw materials as the platinum group materials are. Hence, Pt from membrane electrode assemblies used in the well-known Westinghouse cycle for hydrogen production has been successfully recovered using the selective electrochemical dissolution process and reaching global efficiencies of 70 wt%. Pt electrocatalysts were synthesized from the Pt recovered from the spent electrodes and characterized. Thus, the scanning electrochemical microscopy technique demonstrated that Pt was well dispersed onto the carbon support. Moreover, electrodes with both, commercial and recovered Pt/C catalysts were prepared and tested. The electrodes with the catalyst prepared from the spent MEAs show a good activity towards the SO_2 oxidation, the reaction for H_2 production, and above all, a very high stability. In conclusion, the circular economy of Pt based catalyst for a H_2 production process has been achieved.

1. Introduction

New circular approaches (make, use, return) are increasing in influence and significance with global economic growth. Within industry, closed-loop, circular value chains and sustainable manufacturing are being increasingly recognized as the right path to take in the next years in order to minimize the impact on the planet and preserve strategic natural resources. A fast transition to more sustainable technologies, not only for energy generation, but also for the transportation field, requires a large number of materials such as lithium, cobalt, graphite, rare earths, and platinum's group metals (PGM's), among others, that are unevenly distributed along the planet and are extremely rare [1]. Moreover, our world is facing big energetic and environmental problems which force to move towards renewable energy resources. In this sense, the European Union (EU), for instance, is strongly supporting the Hydrogen technologies in their last research program also known as the European Green deal [2], ranging from electrolyzers to fuel cells. H_2 is nowadays living again a great expectation and most European countries have adopted hydrogen road maps to reach the EU Green deal where the production of green hydrogen (the one produced using renewable energy sources) plays a paramount role. It is well known that the main way for the production of high tons of hydrogen is from steam reforming while less than 5% of hydrogen is produced from renewable sources [3]. Thus, scaling up and developing other hydrogen production technologies such as thermochemical water splitting cycles in an integrated and environmentally friendly way for large-scale hydrogen production can promote hydrogen economy and sustainable development. Among the different thermochemical cycles that exist, one of the most promising is the Hybrid sulfur thermochemical cycle (also called Westinghouse, WH), due to its high thermal efficiency, around 40%. [4]. Furthermore, green hydrogen can be produced by coupling the later mentioned process with concentrated solar energy for the thermochemical step (chemical decomposition of sulfuric acid according to Eq. 1) and solar photovoltaic energy for the SO_2 depolarized electrolysis (hydrogen production according to Eq. 2). This process has the advantage, compared to the direct water electrolysis, that it requires much lower input energy according to its standard potential (0.158 V vs 1.23 V for water electrolysis) [5–8].

$$H_2SO_4 \rightarrow SO_2 + \frac{1}{2}O_2 + H_2O \quad (1)$$

$$SO_2 + 2H_2O \rightarrow H_2SO_4 + 2H^+ + 2e^- \quad (2)$$

On the other hand, recent events have put Europe's sovereignty and competitiveness at risk, so for guaranteeing metals for the chemical

* Corresponding author.
E-mail address: justo.lobato@uclm.es (J. Lobato).

https://doi.org/10.1016/j.apcatb.2023.122414
Received 28 September 2022; Received in revised form 21 December 2022; Accepted 22 January 2023
Available online 24 January 2023

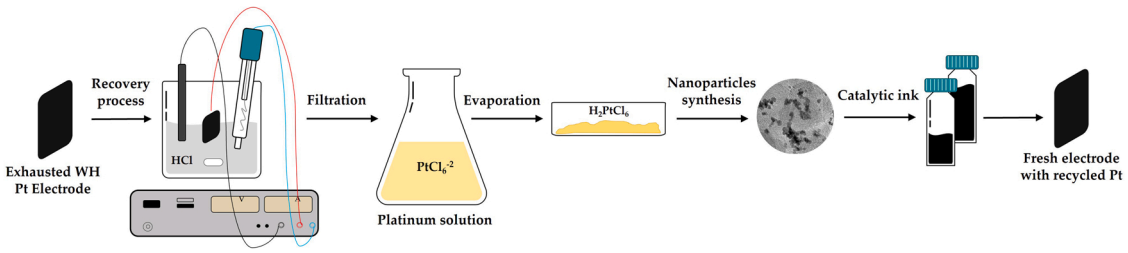

Fig. 1. Scheme of the Pt recovery and re-use.

industry, increasing *in-house* metal recycling is imperative. Underpinning this, the EU just emphasized [9] the urgent need to address *strategic foreign dependencies* for the most critical risks and vulnerabilities, via sustainable recycling, extracting, and processing within the EU. This includes critical raw materials and highlights Mo and W amongst the most vulnerable chemicals. In addition, PGMs (especially Pd) and Ni (i.e., export bans + record high prices) are also struggling with supply problems and price increase [10].

In terms of recycling, current practices are mostly centralized (take-back system by catalyst manufacturers) and dominated by highly intensive and carbon-polluting pyro-/hydro-metallurgical methods, treating spent metal-based catalysts in large volumes, mixed catalyst types, at high metal concentrations or similar chemistries [11]. Conversely, as many waste catalysts do not meet these requirements—necessary for economic profit of existing technologies, they are often landfilled. Thus, in Europe, catalyst production and metal recycling processes must shift to sustainable options, such as the decentralized, flexible recycling and simultaneous downstream synthesis of metal-based catalysts using less-intensive technologies, powered by renewable energies [12].

Electrochemistry already provides the only cost-effective way to obtain certain materials, e.g., there are no alternative technologies for most elements obtained by electrowinning. Therefore, there is a window of opportunity for electrochemistry to play a more significant role in synthesizing and recycling catalysts. From all electrochemical techniques, the selective electrochemical dissolution (SED) of metals using cyclic voltammetry has been proven as an appropriate way to separate refractory metals (Pt, Pd, among others) from the catalyst support with high efficiencies, low energy consumption and avoiding the use of high quantities of chemicals, which often are highly corrosive and hard to manipulate due to the formation of toxic fumes during the operation [13–15]. During past few years, it has been demonstrated that potential cycling is mandatory to prevent the formation of refractory species over the Pt surface than can halt the recovery process [16]. These findings have been pushed to the edge using electroless with electrolyte substitution to modify the Pt surface potential and favor the formation of Pt complexes [17]. Moreover, it has been demonstrated that species like Cl^- and O_2 play a fundamental role on the Pt stripping due to its complexation ability. These findings led to recovery processes on MEA from fuel cells using Pt that can also preserve the carbon support [18]. In conclusion, this method is feasible and user friendly by using a potential control and dilute acidic solutions to efficiently recover Pt catalysts [19]. Also, it could be considered environmentally friendly as the power supply can proceed from renewable energy sources.

In this sense, the current manuscript shows, for the first time, the study of the recycle of spent Pt catalyst from membrane electrode assemblies (MEAs) used in the depolarized SO_2 electrolysis (Eq. 2) for hydrogen production of the Westinghouse cycle using an electrochemical method and the synthesis of fresh Pt catalyst from the recycled one and its use for the same application, reaching in this way a circular economy for Pt catalysts.

2. Experimental

2.1. Analysis of Pt content and physicochemical characterization

The recovered platinum content was determined by ultraviolet (UV)-visible spectrophotometry using an Agilent 300 Cary series UV-Vis spectrophotometer measuring the signal at 263 nm, and by inductively couple plasma optical emission spectrometry (ICP-OES) using a Varian Liberty RL spectrometer. After selective electrochemical dissolution, the electrodes were subjected to acid digestion process using aqua regia (HCl/HNO_3) in a 3:1 ratio (all reagents from Panreac used as received) to dissolve the remaining Pt and close the mass balance. The electrolytes were prepared by diluting the concentrated acids (H_2SO_4 and HCl, Merck) using ultrapure water (mili-Q; resistance > 18.2 MΩ) when required.

TEM micrographs were employed to analyse the Pt dispersion and the size of the catalyst nanoparticles. A Jeol 2100, working at 200 kV, with a double-twist sample holder, (± 30°) and EDS (Oxford Ling) was used for this analysis. To prepare the samples, they were dispersed in acetone and then a drop was deposited on a copper rack covered with perforated C (holey carbon, EMS). On the other hand, XRD analysis were performed by means of a Philips PW-1700 diffractometer equipped with CuKα radiation. The 2θ angular regions between 5° and 90° were studied with a scan rate of $0.1°s^{-1}$. The Scherrer equation was used to calculate the platinum crystallite size (Eq. 3):

$$L_C = \frac{0.89\lambda}{\beta\cos(\theta)} \tag{3}$$

where L_C is the crystallite size in nm, λ corresponds to the Kα radiation of copper (λ = 0.15418 nm), β is a parameter related to the full width at half maximum intensity of the peak, and θ is the angle corresponding to I_{max}(rad). The selected angular region to properly calculate the nanoparticle size were 68º (Pt 220) according to previous works developed by our group [20,21].

Spent electrodes from the MEA used in the Westinghouse cycle were analyzed on energy-dispersive X-ray (EDX) spectroscopy coupled to SEM equipment. The elemental chemical composition of the layers of the electrodes was studied through Analyses were performed using a JEOL JCM 5700 at a 10 kV voltage with 80000x magnification.

2.2. Pt recovery

SED process was used to strip Pt from the used electrodes (5 ×5 cm^2) that were previously used in the WH process for more than 4 h at high temperature (100–150 °C), and thus contaminated with S. Electrodes with a Pt loading: ~0.7 $mg{\cdot}cm^{-2}$ were the case of study for Pt recovery. Each MEA, composed by two electrodes and one PBI based membrane were separated using physical methods and resized to 4 × 4 cm^2 to adapt to the electrochemical cell. The membrane along with the Pt/C catalyst that could not be properly detached were dissolved in hot aqua regia and measured with ICP to quantify the Pt and close the whole mass balance. All the recovery percentages claimed in this work will be referred to the initial loading described of 0.7 $mg{\cdot}cm^{-2}$. Electrochemical

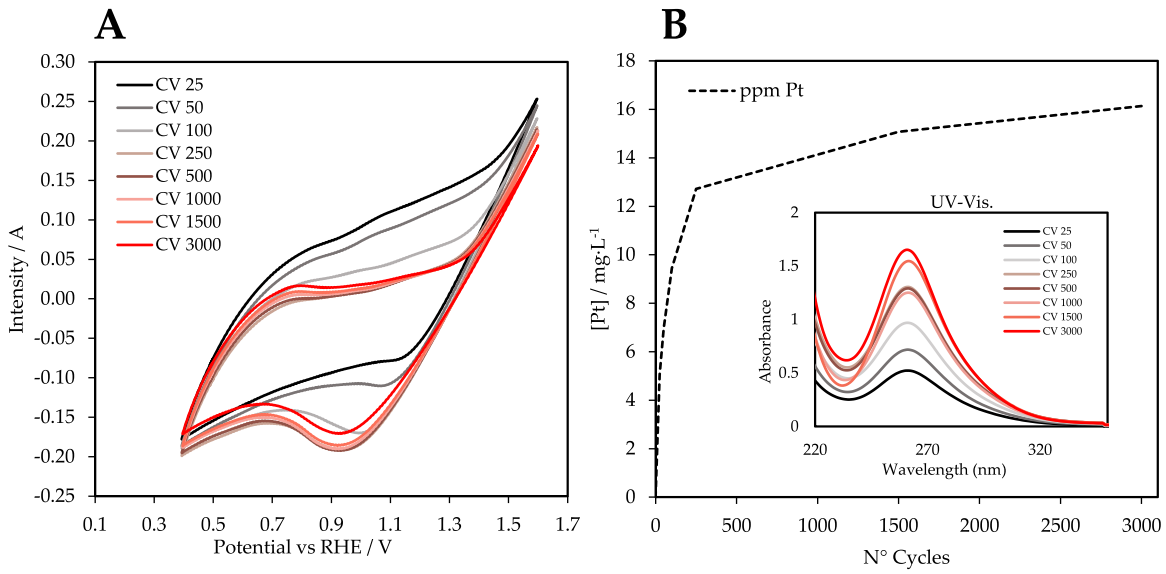

Fig. 2. Cyclic voltammetry of an exhausted Pt electrode from Westinghouse cycle in 0.1 M HCl solution at 50 $mV{\cdot}s^{-1}$ and room temperature. Different cycles were represented (A). Fig. 2B shows the concentration of Pt extracted from the electrode versus the number of CV cycle measured by UV-Vis (inset).

measurements were carried out on an Autolab potensiostat/galvanostat (PGSTAT-302 N). Graphite rod (6 mm Ø) and Ag/AgCl electrodes were used as the counter and reference electrodes, respectively. The used electrodes were electrochemically treated in a solution of HCl (1 M) under agitation for 3000 cycles between 0.4 and 1.6 V vs RHE with a scan rate 50 $mV{\cdot}s^{-1}$. After the SED process, the electrodes were treated with hot aqua regia, and the resulting solution was analysed by ICP to quantify the Pt that remains on the electrode after the treatment. In all cases studied, this value is almost negligible.

2.3. Synthesis of Pt based catalyst

The recovered acidic platinum solution (H_2PtCl_6) from SED was filtered and concentrated by evaporation (see Fig. 1). With the recovered solid, a 0.1 M solution was prepared to synthesize Pt/C nanoparticles with reverse microemulsion method. This is a well-known method to prepare nanoparticulated materials, and particularly Pt nanoparticles, that can be found elsewhere [22,23]. The catalytic ink used to further prepare the electrodes, was done by mixing the recycled Pt/C nanoparticles with Polybenzimidazole ionomer (1.98 wt% PBI in N, N dimethylacetamide, DMAc) in DMAc solvent. The mass fraction of PBI accounts for about 1/20 of the mass of the catalyst support. DMAc was added to adjust the viscosity and surface tension of the catalyst ink and to maintain the dissolution of PBI. PBI ionomer was added to improve adhesion of the film to the electrode surface and to improve the proton conductivity. Before spraying, the catalyst suspension was stirred in an ultrasonic bath for 1 h to ensure sufficient dispersion of the catalyst particles. Catalytic ink was deposited onto commercial carbon paper electrodes (Freudenberg Vliesstoffe H23C2) by spray-gun method to achieve a Pt loading of 0.1 $mg{\cdot}cm^{-2}$.

2.4. Electrochemical characterization of the synthesized and commercial Pt/C electrodes

Electrochemical measurements for the recycled and commercial Pt based electrodes (for comparison purposes) were carried out on an Autolab potentiostat/galvanostat (PGSTAT-302 N) equipped with SCANGEN 250 that allows to perform linear voltammetry. Carbon paper and Ag/AgCl electrodes were used as the counter and reference electrodes, respectively. Cyclic voltammetry experiments were carried out in a half-cell to evaluate the electrochemical surface-active area (ECSA) before each experiment, calculated through the H_2 desorption peak area, using Eq. (4):

$$ECSA = \frac{A_{(Pt)}}{\upsilon x C} x \frac{1}{L} \quad (4)$$

where $A_{(Pt)}$ is the surface under the hydrogen desorption peak (AV cm^{-2}), υ is the scan rate (V s^{-1}), C is a constant related to the required load required to reduce the proton layer on the active platinum (0.21 mC cm^{-2}) and L is the platinum loading in the catalyst layer (in our case, it was 0.1 mgPt cm^{-2}).

On the other hand, to evaluate the stability and activity of the platinum electrodes, chronoamperometry (CA) and linear sweep voltammetry (LSV) tests were performed in a half-cell in which SO_2 was bubbled for 1 min in a 0.5 M H_2SO_4 solution, and after that, a potential of 0.977 V vs RHE was applied for 4 h for the CA experiments and a potential sweep from 0.2 to 1 V vs RHE at 10 mV/s was used to perform LSV measurements [19]. These techniques were applied to both the recovered and commercial Pt catalyst.

Scanning Electrochemical Microscope (SECM) experiments were performed using a Sensolytics SECM-103. Briefly, a one electrode electrochemical mediator ($K_3Fe(CN)_6$, Merck 99%) was used as a probe to estimate the distance between a Pt microelectrode (25 μm of diameter) and the electrode surface. Prior to the imaging of the surface, approach curves must be made for (X,Y,Z) directions to set the initial distance of the microelectrode to the surface (Z) and to prevent any collision of the microelectrode with the surface (X,Y). To perform these curves, the Pt microelectrode potential was set to − 0.1 V vs Ag/AgCl in a 10 mM $K_3Fe(CN)_6$ solution to achieve an Iss (stationary state current) at the same time that the microelectrode moves towards the surface. This Iss current changes when the microelectrode is near enough to the surface. If the material at the surface is able to regenerate the mediator, a positive feedback response is achieved (increase of current), on the contrary if it is not, a negative feedback profile appears (decrease of the current due to diffusion restrictions near the surface). In this case, Pt/C electrodes give a positive feedback response, while bare Carbon electrodes gives a negative feedback response. Although a pure positive feedback response is not obtained due to the carbon matrix, a relation between increasing or decreasing current and the distance to the surface can be made [24]. After that, a 1 × 1 mm image was taken in the fast-comb mode data acquisition, that consists in moving the Pt microelectrode along X and Y directions with increments of 25 μm and keeping Z value constant. In

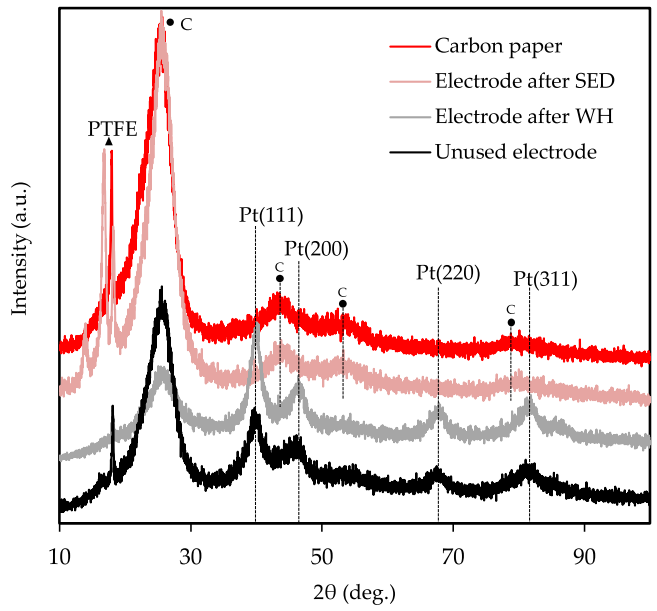

Fig. 3. XRD patterns of an unused Pt/C electrode, an exhausted Pt electrode after being used in the Westinghouse process, an electrode after the SED recovery method, and a pristine carbon paper.

each increment a current sample was taken to form the SECM image once all samples are combined. The current obtained in each point were converted to distance to the surface with a semi-empirical method using the approach curves done for the Z axis. After that, the resulting image was processed with Gwyddion to minimize noise as much as possible.

3. Results and discussions

3.1. Platinum recovery

Fig. 2A shows the SED performed to a Pt/C electrode previously used in the Westinghouse cycle. Briefly, a $4 \times 4\ cm^2$ piece was cut and immersed in an electrochemical cell filled with 1 M HCl, after that, 3000 electrochemical cycles between 0.4 and 1.6 V vs RHE were applied in air atmosphere under stirring. Although, 1.6 V favours the carbon corrosion, this high value potential was selected to obtain a high dissolution rate of Pt particles as it has been stated by Sharma et al. [19]. In the first cycles (black and grey lines), intense oxidation signals were obtained between 0.5 and 1.3 V, which correspond to Pt oxidation. From cycle 500–3000 this signal drops dramatically indicating that probably more Pt was already stripped from the electrode. In addition, the oxidation current observed beyond 1.3 V corresponds mainly to the oxidation of the carbon support and the generation of Cl_2 from the Cl^- present in the electrolyte. Both electrochemical oxidation of Pt in presence of Cl^- and the generation of Cl_2 in an oxidative environment (presence of O_2) are responsible of the efficient Pt stripping. At the same time, a reduction signal grows at a potential around 1 V, probably due to the reduction of species generated during the oxidation of chloride species or the carbon support itself. These findings agree with the measured Pt content of the solution (Fig. 2B) in which Pt concentration rises fast up to 500 cycles. After that, a steadier increasing is observed, this may indicate that the smaller and more accessible particles are dissolved first, while other Pt nanoparticles, which are bigger and/or occluded within the carbon structure, need more time to be leached. Moreover, it can be said that the electrochemical dissolution of Pt takes place mainly through the formation of $[PtCl_4]^{2-}$ species because the absorption peak was spotted at 265 nm approx. [19].

To support the voltametric data, XRD analysis were done to a bare carbon paper, an unused Pt/C electrode, an electrode used in the Westinghouse reaction, and an electrode after the SED process. XRD patterns are shown in Fig. 3. Pt signals can be seen in both the fresh and used in Westinghouse cycle electrodes, while the profile of the electrode after SED is coincident with the carbon paper, proving that no Pt remains on the electrode after the SED process. Moreover, with the XRD signals of Pt and using the Eq. 3, the size of the Pt nanoparticles can be estimated for the unused Pt/C electrode and the electrode used in the Westinghouse process. Data plotted in Table 1 indicate that the pristine Pt nanoparticles, sized in approximately 2.66 nm (coincident with the value given by the supplier), undergo a degradation process that include the coalescence and the dissolution-reprecipitation to increase their size to 3.60–3.80 nm after being used in the Westinghouse process. These degradation mechanisms have been extensively demonstrated for the operational range of fuel cells and similar electrochemical conditions for Pt nanoparticulated catalysts [19,25–27].

Table 1
Nanocrystal size estimation using XRD patterns and Scherrer equation for an unused Pt electrode and after being used in the Westinghouse (WH) process (anodic and cathodic electrodes).

Pt Crystallite size (nm)		
Unused electrode	**Anode after WH**	**Cathode after WH**
2.66	3.64	3.85

In addition, it should be remarked that the electrodes used in this work have been used for the study of the SO_2 depolarized electrolysis at high temperature where the presence of sulfur based species in both electrodes are present [28,29]. This is confirmed by the SEM-EDX analysis performed to both electrodes (anode and cathode) and showed in Fig. S1 and Table S1 of the supplemental material of this manuscript. Hence, it can be claimed that the SDE process using our

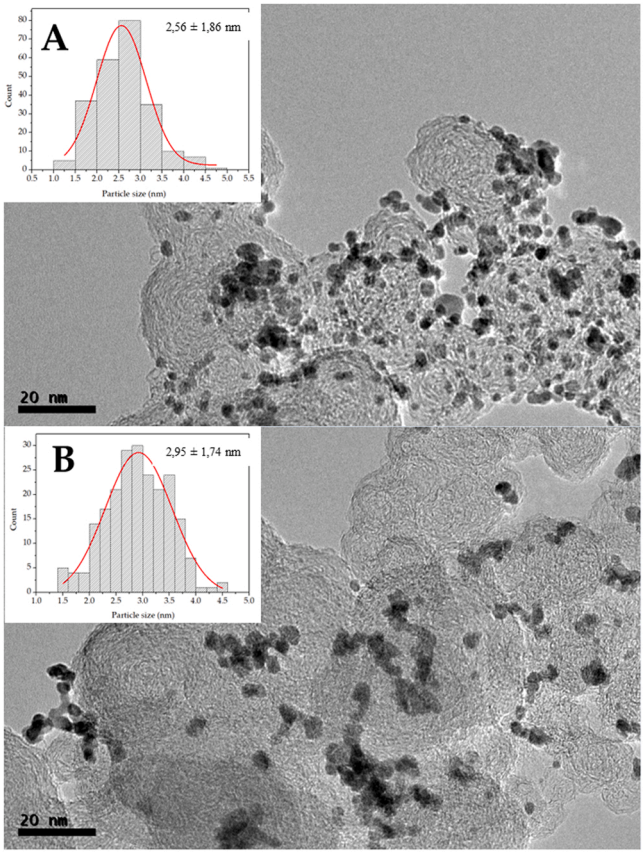

Fig. 4. TEM images of Pt commercial Pt/C catalyst (A) and Pt/C catalyst synthesized in the laboratory with recovered Pt (B). Insets show particle size distribution.

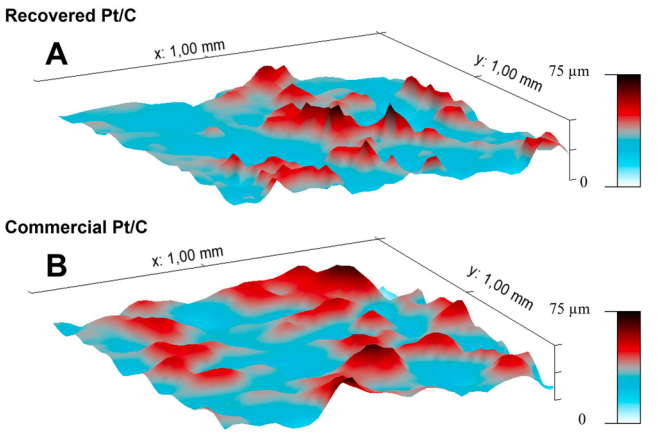

Fig. 5. Fast comb SEMC images of 1 × 1 mm section of recovered (A) and commercial Pt/C electrodes (B). The color scale represents the surface profile of each sample in terms of height (microns).

operation conditions is suitable for the electrochemical dissolution of Pt. And, as it will be explained below, the S based species did not prevent that Pt based electrocatalysts could be prepared with high activity and stability.

3.2. Synthesis of Pt/C catalyst with recovered Pt

Once the SED is finished, the final concentration of the Pt solution is determined to calculate the total recovery of Pt from the used Pt/C electrode. Several samples corresponding to 6 different recovery processes were measured by UV/Vis giving a recovery of 70.1 ± 4.3%. Despite being a viable value to valorise Pt, is far from other SED studies where over 90% of the Pt was leached [30]. However, when ICP measurements were done, a value of 90.3 ± 4.6% of recovered Pt was obtained. This increase when measuring with ICP must be due to the quantification of non-ionic Pt, in other words, Pt nanoparticles that detached from the electrode due to the carbon matrix degradation over the voltametric cycles. Furthermore, the process of detaching the MEA involves a loss of Pt that remains anchored to the membrane, this Pt value was 5.2 ± 1.9% of the initial Pt content. On the other hand, the complete recycling of the Pt means the fabrication of new Pt/C electrodes for their further use in the Westinghouse process. For that purpose, Pt/C nanoparticles were prepared following the procedure described in the experimental section. The target Pt content at the Pt/C catalyst were 40 wt% and the obtained Pt/C catalyst show a Pt value of 39.5 ± 0.4 wt% measured by ICP, and thus with an efficiency of 98.8%. The slight deviation from the theoretical value could be ought to the water absorption of the Pt precursor during the synthesis process. After including the synthesis efficiency to the recovery efficiency of the SED, the global process efficiency (recovery and re-synthesis [31] is 69.3 ± 4.4%. On the other hand, Fig. 4 shows the TEM images of the synthesized nanoparticles (4B), and are compared to the commercial Pt/C catalyst used in the fabrication of the electrodes (4 A). TEM images indicate that the catalyst prepared with the recovered Pt is not as well dispersed over the carbon support as the commercial ones. Also, the size of the nanoparticles is different, while the commercial ones have a size of 2.56 ± 1.86 nm, the synthesized Pt nanoparticles size is 2.95 ± 1.74 nm. Nevertheless, it can be concluded that the catalyst prepared from the recovered Pt have an appropriate dispersion and particle size to be used for the intended electrochemical applications. Thus, other Pt based catalysts used for high temperature proton exchange membrane fuel cells have shown lower dispersion an even higher Pt particle size [32,33].

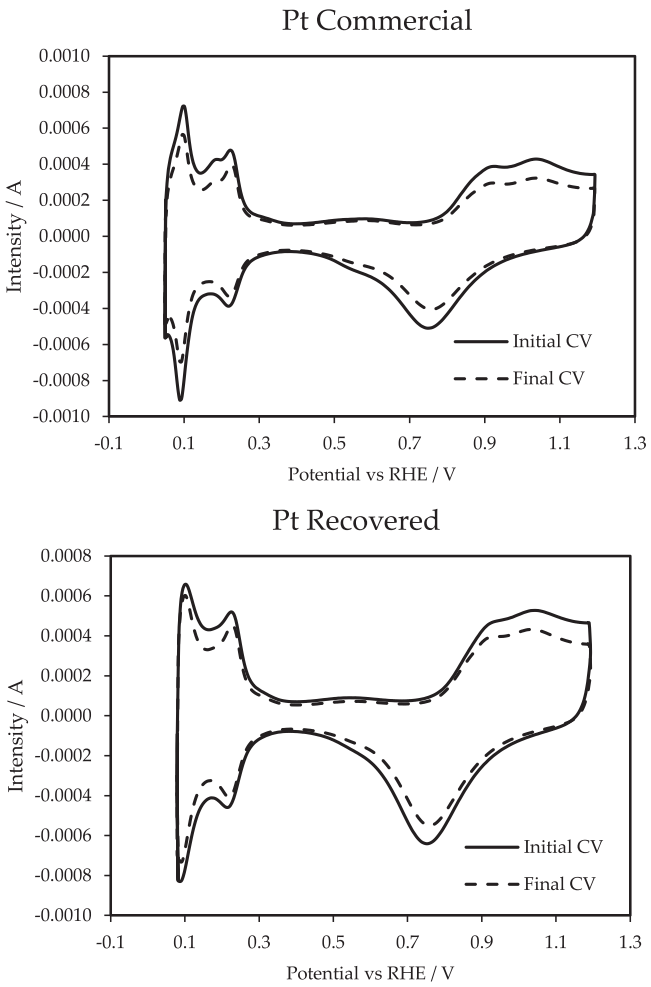

Fig. 6. Cyclic voltammetry of an unused electrode of commercial Pt/C nanoparticles (A) and an unused electrode of Pt/C nanoparticles made with recovered Pt (B) in H_2SO_4 0.5 M. Initial scan (black line) and scan 500 (dashed line) were compared. Pt counter electrode and Ag/AgCl reference electrode were used.

3.3. Electrochemical characterization of synthesized Pt/C recovered catalyst

Two Pt/C (40% wt of Pt on Vulcan carbon support) based electrodes were prepared using commercial Pt/C nanoparticles and recovered Pt/C nanoparticles by airbrushing a catalytic ink over carbon paper electrodes (see experimental section) up to a Pt loading of 0.1 mg·cm^{-2}. SECM was used to evaluate the surface morphology and the Pt distribution along the support. Fig. 5 shows that both recovered and commercial Pt/C electrodes present a similar surface morphology, that corresponds to the one expected from an airbrushing deposition process. Positive feedback is achieved in both electrodes, which suggests that the Pt is well dispersed along the carbon support and the surface, at least enough to the resolution of this particular experiment (25 µm, dependent on the microelectrode diameter). Briefly, blue/red scale represents the surface height with respect to the initial reference point taken of the image (upper left corner). Red parts, in which the current rise due positive feedback, indicates that the surface gets closer to the microelectrode tip, thus presenting a positive protuberance, probably due to the airbrushing process. The order of magnitude of the electrode mapping is around 0–75 µm on the higher hills and no pattern is found, which is expected for a hand-made process like airbrush is. Hence, this technique also confirms what it was also observed by the TEM images, where the Pt nanoparticles are dispersed well enough to be used as

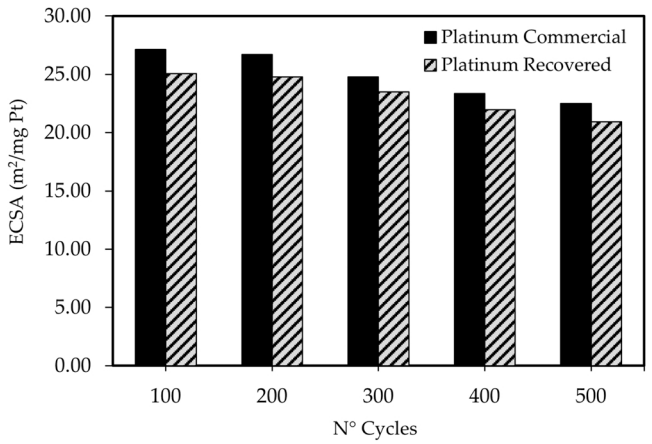

Fig. 7. Calculated Pt electrochemical area (ESCA) for Pt/C nanoparticulated commercial (black) and recovered (stripes) electrode at different voltametric cycles.

catalyst for electrochemical applications.

On the other hand, linear cyclic voltammetry was performed to study the electrochemical active area of the two 0.1 mg·cm^{-1} Pt loading electrodes (prepared with commercial and recovered Pt). Fig. 6 shows the electrochemical profiles where a typical Pt nanoparticle response is obtained for both electrodes [22]. However, the peak definition of the commercial electrode is better, probably due to the differences in the synthetic route of the Pt/C nanoparticles and their size as seen in TEM images. To evaluate the stability of both catalysts, 500 cycles were carried out, and the variation of the ECSA with the number of cycles was used as indicative parameter of the stability of the electrodes. Fig. 7 summarizes all values obtained and as it can be seen, the area loss along the cycles is almost the same in both electrodes, being 17.0% and 16.4% for commercial and recovered electrodes, respectively. Moreover, both electrodes perform similarly during the first 200 cycles as the ECSA values slightly changed, and the main ECSA loss started after 300 cycles in both electrodes. This area loss is due to dissolution-reprecipitation of Pt, catalyst fouling, and nanoparticle coalescence. On the other hand, the area obtained per mg of Pt is very similar for the two electrodes, being slightly higher in the commercial Pt/C particles, probably due to the smaller particle size and better dispersion of the Pt nanoparticles. Although these findings, the recovered Pt/C catalyst reaches proper area values to its use as catalyst for the Westinghouse process. These results point out that the electrochemical method used for Pt recovery is valid and allows the use of the recovered Pt for the preparation of electrocatalysts.

To assess the catalytic activity towards SO_2 oxidation for hydrogen production, a key reaction in the Westinghouse cycle, both a LSV between 0.1 and 1 V and a chronoamperometry at 0.977 vs RHE for 4 h were applied in a SO_2 saturated H_2SO_4 0.5 M solution. Fig. 8 depicts the behavior for both commercial (grey) and recovered (black) Pt/C electrodes. In both cases, commercial Pt electrode exhibits higher initial activity per gram of Pt and decays over time rapidly in the case of the chronoamperometry, while the recovered Pt electrode starts at a lower activity, but its decay is slower, exhibiting a higher activity for SO_2 oxidation after 1 h of operation. This initial higher activity of the commercial electrode is confirmed by both techniques LSV and CA. This behavior could be mostly due to the initial state of both catalysts. Commercial Pt/C has a smaller nanoparticle size, and it is better dispersed (see TEM images), which could explain the activity loss caused by dissolution-reprecipitation and nanoparticle coalescence, while the recovered Pt/C already has bigger nanoparticle size and has a worse dispersion compared with the commercial one, so these degradation processes have less impact in the activity. According to this data, the recovered Pt/C catalyst is a promising candidate to complete the recovery Pt cycle and be used in the Westinghouse process.

4. Conclusions

In this work, electrodes based on Pt electrocatalysts synthesized from Pt recovered from spent MEA of the Westinghouse cycle for hydrogen production have been prepared, characterized and tested for the initial application, i.e. sulfur depolarized electrolysis.

The main conclusions that can be drawn are:

-The SED technique is a feasible technique that allows to recover the Pt from spent MEAs with high global efficiency up to 70% wt under our operation conditions despite the electrodes were contaminated with sulfur species.

- 40% wt Pt/C electrocatalyst from the Pt recovered has been successfully synthesized.

- The synthesized Pt based electrocatalysts shows a good dispersion and Pt particle size. Moreover, the electrochemical tests conclude that the synthesized electrocatalyst shows a good activity towards the SO_2 oxidation (a reaction for H_2 production) and above all a very high electrochemical stability.

Finally, in this work, the circular economy of Pt catalyst for hydrogen production has been demonstrated which makes the H_2 production can be more sustainable if Pt catalysts are recovered and reused.

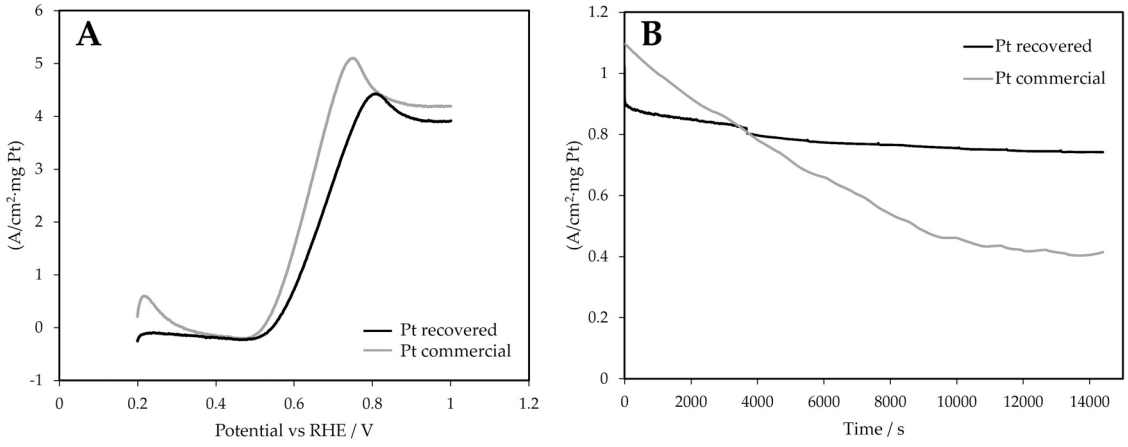

Fig. 8. A) LSVs of commercial (grey) and recovered (black), in SO_2-bubbled 0.5 M H_2SO_4 between 0.2 and 1.2 V vs RHE at 10 mV/s and B) Chronoamperometry of commercial (grey) and recovered (black) Pt/C nanoparticulated electrodes in a SO_2 saturated H_2SO_4 0.5 M solution at 0.977 V vs RHE for 4 h. Carbon paper and Ag/AgCl were used as counter and reference electrodes, respectively.

CRediT authorship contribution statement

Miguel A. Montiel: Investigation, Conceptualization, Data curation, Writing - original draft. **Rafael Granados-Fernández:** Investigation, Data curation, Writing - original draft. **Sergio Díaz-Abad:** Writing – original draft, Investigation. **Cristina Sáez:** Writing – review & editing. **Carmen M. Fernández-Marchante:** Writing – review & editing, Supervision. **Manuel A. Rodrigo:** Funding acquisition, Project administration. **Justo Lobato:** Writing – original draft, Supervision, Conceptualization, Project administration, Funding acquisition.

Declaration of Competing Interest

The authors declare that they have no known competing financial interests or personal relationships that could have appeared to influence the work reported in this paper.

Data Availability

Data will be made available on request.

Acknowledgements

Miguel A. Montiel is grateful to the Spanish Ministry of Science and Innovation for his postdoctoral fellowship, Juan de la Cierva Formación Program (FJC2019-039279-I). This work also belongs to the project PID2019-107271RB-I00 granted by MCIN/ AEI/10.13039/ 501100011033/ and "Unión Europea NextGenerationEU/PRTR" and the project ASEPHAM. Grant number "SBPLY/17/180501/000330" funded by the Junta de Comunidades de Castilla-La Mancha and the FEDER and EU Program. Therefore, these Institutions are gratefully acknowledged. Sergio Diaz also acknowledges the grant 2018/12504 from University of Castilla-La Mancha.

Appendix A. Supporting information

Supplementary data associated with this article can be found in the online version at doi:10.1016/j.apcatb.2023.122414.

References

[1] IPCC, Global Warming of 1.5°C: IPCC Special Report on Impacts of Global Warming of 1.5°C above Pre-industrial Levels in Context of Strengthening Response to Climate Change, Sustainable Development, and Efforts to Eradicate Poverty, Cambridge University Press, Cambridge, 2022. https://doi.org/DOI: 10.1017/9781009157940.
[2] European Commission, The European Green Deal, Eur. Comm. 53 (2019) 24. https://doi.org/10.1017/CBO9781107415324.004.
[3] I. Dincer, C. Zamfirescu, Sustainable hydrogen production options and the role of IAHE, Int. J. Hydrog. Energy 37 (2012) 16266–16286, https://doi.org/10.1016/j.ijhydene.2012.02.133.
[4] E. Bilgen, Solar hydrogen production by hybrid thermochemical processes, Sol. Energy 41 (1988) 199–206, https://doi.org/DOI. 10.1016/0038-092X(88)90137-5.
[5] S. Díaz-Abad, M. Millán, M.A. Rodrigo, J. Lobato, Review of anodic catalysts for SO2 depolarized electrolysis for "green hydrogen" production, Catalysts 9 (2019), https://doi.org/10.3390/catal9010063.
[6] S. Díaz-Abad, M.A. Rodrigo, J. Lobato, First approaches for hydrogen production by the depolarized electrolysis of SO2 using phosphoric acid doped polybenzimidazole membranes, Int. J. Hydrog. Energy 46 (2021) 29763–29773, https://doi.org/10.1016/j.ijhydene.2021.06.117.
[7] B.H. Meekins, A.B. Thompson, V. Gopal, B.A.T. Mehrabadi, M.C. Elvington, P. Ganesan, T.A. Newhouse-Illige, A.W. Shepard, L.E. Scipioni, J.A. Greer, J. C. Weiss, J.W. Weidner, H.R. Colón-Mercado, In-situ and ex-situ comparison of the electrochemical oxidation of SO2 on carbon supported Pt and Au catalysts, Int. J. Hydrog. Energy 45 (2020) 1940–1947, https://doi.org/10.1016/j.ijhydene.2019.11.112.
[8] A. Nadar, A.M. Banerjee, M.R. Pai, S.S. Meena, R.V. Pai, R. Tewari, S.M. Yusuf, A. K. Tripathi, S.R. Bharadwaj, Nanostructured Fe2O3 dispersed on SiO2 as catalyst for high temperature sulfuric acid decomposition—structural and morphological modifications on catalytic use and relevance of Fe2O3-SiO2 interactions, Appl. Catal. B Environ. 217 (2017) 154–168, https://doi.org/10.1016/j.apcatb.2017.05.045.
[9] European Commission, COMMUNICATION FROM THE COMMISSION TO THE EUROPEAN PARLIAMENT, THE EUROPEAN COUNCIL, THE COUNCIL, THE EUROPEAN ECONOMIC AND SOCIAL COMMITTEE AND THE COMMITTEE OF THE REGIONS, Eur. Comm. (2022). https://eur-lex.europa.eu/legal-content/EN/TXT/?uri=CELEX%3A52022PC0247.
[10] L. Grandell, A. Lehtilä, M. Kivinen, T. Koljonen, S. Kihlman, L.S. Lauri, Role of critical metals in the future markets of clean energy technologies, Renew. Energy 95 (2016) 53–62, https://doi.org/10.1016/j.renene.2016.03.102.
[11] K.D. Rasmussen, H. Wenzel, C. Bangs, E. Petavratzi, G. Liu, Platinum demand and potential bottlenecks in the global green transition: a dynamic material flow analysis, Environ. Sci. Technol. (2019), https://doi.org/10.1021/acs.est.9b01912.
[12] M. Marafi, A. Stanislaus, Spent catalyst waste management: a review. Part I-Developments in hydroprocessing catalyst waste reduction and use, Resour. Conserv. Recycl 52 (2008) 859–873, https://doi.org/10.1016/j.resconrec.2008.02.004.
[13] R. Granados-Fernández, M.A. Montiel, S. Díaz-Abad, M.A. Rodrigo, J. Lobato, Platinum recovery techniques for a circular economy, Catalysts 11 (2021), https://doi.org/10.3390/catal11080937.
[14] H. Dong, J. Zhao, J. Chen, Y. Wu, B. Li, Recovery of platinum group metals from spent catalysts: a review, Int. J. Miner. Process. 145 (2015) 108–113, https://doi.org/10.1016/j.minpro.2015.06.009.
[15] J. Cui, L. Zhang, Metallurgical recovery of metals from electronic waste: a review, J. Hazard. Mater. 158 (2008) 228–256, https://doi.org/10.1016/j.jhazmat.2008.02.001.
[16] H. Shiroishi, S. Hayashi, M. Yonekawa, R. Shoji, I. Kato, M. Kunimatsu, Dissolution rate of noble metals for electrochemical recycle in polymer electrolyte fuel cells, Electrochemistry 80 (2012) 898–903, https://doi.org/10.5796/electrochemistry.80.898.
[17] R. Latsuzbaia, E. Negro, G.J.M. Koper, Environmentally friendly carbon-preserving recovery of noble metals from supported fuel cell catalysts, ChemSusChem 8 (2015) 1926–1934, https://doi.org/10.1002/cssc.201500019.
[18] R. Sharma, P. Morgen, S.M. Andersen, Platinum recycling through electroless dissolution under mild conditions using a surface activation assisted Pt-complexing approach, Phys. Chem. Chem. Phys. 22 (2020) 13030–13040, https://doi.org/10.1039/c9cp06066a.
[19] R. Sharma, K. RodeNielsen, P. BrilnerLund, S. BredmoseSimonsen, L. Grahl-Madsen, S. MaAndersen, Sustainable platinum recycling through electrochemical dissolution of platinum nanoparticles from fuel cell electrodes, ChemElectroChem 6 (2019) 4471–4482, https://doi.org/10.1002/celc.201900846.
[20] J. Lobato, H. Zamora, J. Plaza, P. Cañizares, M.A. Rodrigo, Enhancement of high temperature PEMFC stability using catalysts based on Pt supported on SiC based materials, Appl. Catal. B Environ. 198 (2016) 516–524, https://doi.org/10.1016/j.apcatb.2016.06.011.
[21] J. Lobato, P. Cañizares, M.A. Rodrigo, J.J. Linares, Study of different bimetallic anodic catalysts supported on carbon for a high temperature polybenzimidazole-based direct ethanol fuel cell, Appl. Catal. B Environ. 91 (2009) 269–274, https://doi.org/10.1016/j.apcatb.2009.05.035.
[22] J. Solla-Gullón, V. Montiel, A. Aldaz, J. Clavilier, Electrochemical characterization of platinum nanoparticles prepared by microemulsion: How to clean them without loss of crystalline surface structure, J. Electroanal. Chem. 491 (2000) 69–77, https://doi.org/10.1016/S0022-0728(00)00306-5.
[23] J. Solla-Gullón, V. Montiel, A. Aldaz, J. Clavilier, Synthesis and electrochemical decontamination of platinum-palladium nanoparticles prepared by water-in-oil microemulsion, J. Electrochem. Soc. 150 (2003), E104, https://doi.org/10.1149/1.1534600.
[24] M.V.M. Allen J. Bard, Scanning Electrochemical Microscopyo Title, 2012.
[25] A. Pavlišič, P. Jovanovič, V.S. Šelih, M. Šala, N. Hodnik, M. Gaberšček, Platinum dissolution and redeposition from Pt/C fuel cell electrocatalyst at potential cycling, J. Electrochem. Soc. 165 (2018) F3161–F3165, https://doi.org/10.1149/2.0191806jes.
[26] P. Jovanovič, U. Petek, N. Hodnik, F. Ruiz-Zepeda, M. Gatalo, M. Šala, V.S. Šelih, T. P. Fellinger, M. Gaberšček, Importance of non-intrinsic platinum dissolution in Pt/C composite fuel cell catalysts, Phys. Chem. Chem. Phys. 19 (2017) 21446–21452, https://doi.org/10.1039/c7cp03192k.
[27] A.A. Topalov, I. Katsounaros, M. Auinger, S. Cherevko, J.C. Meier, S.O. Klemm, K. J.J. Mayrhofer, Dissolution of platinum: limits for the deployment of electrochemical energy conversion? Angew. Chem. - Int. Ed. 51 (2012) 12613–12615, https://doi.org/10.1002/anie.201207256.
[28] S. Díaz-Abad, S. Fernández-Mancebo, M.A. Rodrigo, J. Lobato, Enhancement of SO2 high temperature depolarized electrolysis by means of graphene oxide composite polybenzimidazole membranes, J. Clean. Prod. 363 (2022), https://doi.org/10.1016/j.jclepro.2022.132372.
[29] S. Díaz-Abad, M.A. Rodrigo, C. Sáez, J. Lobato, Enhancement of the green H2 production by using TiO2 composite polybenzimidazole membranes, Nanomaterials 12 (2022) 2920, https://doi.org/10.3390/nano12172920.
[30] S. Kanamura, M. Yagyu, Electrochemical dissolution of platinum and ruthenium from membrane electrode assemblies of polymer electrolyte fuel cells, Mater. Trans. 57 (2016) 1972–1976, https://doi.org/10.2320/matertrans.M2016198.
[31] L. Duclos, R. Chattot, L. Dubau, P.X. Thivel, G. Mandil, V. Laforest, M. Bolloli, R. Vincent, L. Svecova, Closing the loop: Life cycle assessment and optimization of

a PEMFC platinum-based catalyst recycling process, Green. Chem. 22 (2020) 1919–1933, https://doi.org/10.1039/c9gc03630j.

[32] J. Lobato, S. Díaz-Abad, M.C. Peláez, M. Millán, M.A. Rodrigo, Synthesis and characterization of Pt on novel catalyst supports for the H2 production in the Westinghouse cycle, Int. J. Hydrog. Energy 45 (2019) 25672–25680, https://doi.org/10.1016/j.ijhydene.2019.10.154.

[33] H. Zamora, J. Plaza, P. Velhac, P. Cañizares, M.A. Rodrigo, J. Lobato, SiCTiC as catalyst support for HT-PEMFCs. Influence of Ti content, Appl. Catal. B Environ. 207 (2017) 244–254, https://doi.org/10.1016/j.apcatb.2017.02.019.